Quantum Information Review
An International Journal

http://dx.doi.org/10.12785/qir/030102

Some Statistical Properties of a Non-linear Entangled Pair Coherent State

A. S. -F. Obada[1], *E. M. Khalil*[1,3,*], *M. A. El-Deberky*[2] *and S. Sanad* [2]

[1] Mathematics Department, Faculty of Science, Al-Azher University, Nasr City 11884, Cairo, Egypt
[2] Mathematics Department, Faculty of Science (Girls Branch), Al-Azher University, Nasr City 11884, Cairo, Egypt
[3] Mathematics Department, Faculty of Science, Taif University, Taif City 888, Saudi Arabia

Received: 1 Dec. 2014, Revised: 20 Dec. 2014, Accepted: 23 Dec.2014
Published online: 1 Jan. 2015

Abstract: A new type of a non-linear entangled pair coherent state is introduced. Under a certain choice of the non-linear functions the solution of the recurrence relation is obtained. Phenomenon of squeezing and the Poissonian distribution are examined. It is shown that the eigenvalue of the photon number sum (the q-parameter) is responsible for some of nonclassical phenomenon. Furthermore, the quasi-probability distribution functions (the Wigner and Q-functions) are discussed. For the Wigner function the nonclassical behaviour is only displayed for odd values of the q-parameter in a restricted subspace. Finally the phase distribution in the framework of Pegg and Barnett formalism is considered.

Keywords: Entangled states, Correlation function, Q-Function, Wigner Function

1 Introduction

The number state $|n\rangle$ represents the corner stone to deal with any problem related to the fields of quantum mechanics and quantum optics [1,2]. In the meantime, the appearance of the coherent state besides the thermal state opened the door to discover other states which have nonclassical properties [2,3,4,5,6]. In this sense one may mention the binomial state, the generalized geometric state and the logarithmic state, etc [7,8,9,10,11]. In fact these states are intermediate states which interpolate between either the number state and the coherent state [7], or between the number state and pure thermal state [9]. However, the logarithmic state can be viewed as an interpolation between the generalized Bose-Einstein states and the coherent state. The above mentioned states are generated from quantum systems which describe kinds of interaction between an atom and a field. For example the binomial state can be generated from a system consisting of the linear combination between two raising and lowering operators related to the angular momentum operators [12,13,14]. While the generalized geometric state can be generated from the Hamiltonian which describes the interaction between multiphoton processes in finite level atomic system [9]. As one can see the above mentioned states are just few of many other intermediate states. Besides these intermediate states there exist other states termed as correlated states [15]. For instance pair coherent states (**PCS**) $|\zeta,q\rangle$ represent an important type of correlated two-mode states which posses prominent nonclassical properties. These states satisfy the following eigenvalue relations

$$\hat{a}_1\hat{a}_2|\zeta,q\rangle=\zeta|\zeta,q\rangle \qquad \text{and} \qquad (\hat{n}_1-\hat{n}_2)\,|\zeta,q\rangle=q|\zeta,q\rangle, \tag{1}$$

where $\hat{a}_i(\hat{a}_i^{\dagger})$ $i=1,2$ are the annihilation (creation) operators and $\hat{n}_i, i=1,2$ are the photon number operators of the two field modes. The parameter q is an integer and ζ may be a complex numbers. Also we may refer to another type of correlated two-mode states that is a finite-dimensional pair coherent state. In analogy to the definition of the pair-coherent state, the finite dimensional **PCS** is defined as the eigenstate of the pair of operators: $\left\{\hat{a}_1^{\dagger}\hat{a}_2+\left(\hat{a}_1\hat{a}_2^{\dagger}\right)^q\zeta^{q+1}/(q!)^2\right\}$ with eigenvalue ζ and the sum of the photon number operators for the two modes $(\hat{n}_1+\hat{n}_2)$ with eigenvalue q. In terms of the number states of the two modes, thus state is given by [16,17]

$$|\zeta,q\rangle=N_q\sum_{n=0}^{q}\zeta^n\sqrt{\frac{(q-n)!}{q!n!}}|q-n,n\rangle, \tag{2}$$

* Corresponding author e-mail: eiedkhalil@yahoo.com

where ζ is a complex parameter and q is an integer and N_q is the a normalization constant, for more details one may consult the above references. In fact the state in the above equation has been introduced during the study of the statistical properties of a two-photon cavity mode in the presence of frequency converter.

As another example may be mentioned in this context, the two mode nondegenerate entangled state. This state is constructed from the eigenstate of the pair operators $(\mu\hat{a}\hat{b}+\nu\hat{a}^{\dagger}\hat{b}^{\dagger}-\sqrt{\mu\nu}(\hat{a}\hat{a}^{\dagger}+\hat{b}^{\dagger}\hat{b}))$ and the difference of the photon number operators $(\hat{n}_a-\hat{n}_b)$ for two modes [18].

In this paper, we address the problem of constructing and discussing some properties of a new correlated two mode states. The results that we are going to present states that stem from an approach to a nonlinear PCS (NLPCS) namely

$$\begin{gathered}(\mu\hat{a}\hat{b}f(\hat{n}_a)f(\hat{n}_b)+\nu f(\hat{n}_a)f(\hat{n}_b)\hat{a}^{\dagger}\hat{b}^{\dagger}\\ -\sqrt{\mu\nu}(\hat{a}\hat{a}^{\dagger}\,(f(\hat{n}_a+1))^2+\hat{b}^{\dagger}\hat{b}\,(f(\hat{n}_b))^2))|\xi,\zeta,q\rangle=\xi|\xi,\zeta,q\rangle,\\ (\hat{a}^{\dagger}\hat{a}-\hat{b}^{\dagger}\hat{b})|\xi,\zeta,q\rangle=q|\xi,\zeta,q\rangle,\end{gathered} \tag{3}$$

where ζ reflects the squeeze parameter which is a result of defining $\mu=\cosh^2\zeta$ and $\nu=\sinh^2\zeta$ and satisfying the condition $\mu-\nu=1$, ξ is a complex parameter of the state while the q parameter is an integer number.

When we choose the non-linear function to take the form $f(\hat{n}_i)=\frac{1}{\sqrt{\hat{n}_i}}, i=a,b$ the state is given by

$$|\xi,\zeta,q\rangle=\sqrt{1-|m|^2}\sum_{n=0}^{\infty}m^n|q+n,n\rangle,$$

$$m=\tanh\zeta\left[(1+\frac{\xi}{\sinh 2\zeta})-\sqrt{(1+\frac{\xi}{\sinh 2\zeta})^2-1}\right] \tag{4}$$

(see Appendix)

Now in figure (1) we plot m against ξ and ζ which shows that for small values of ζ the curve increases slowly but then it shoots to become almost 1. By increasing ξ the curve shoots faster to reach almost its maximum.

It is clear that when $q=0$ the state (4) becomes two mode vacuum state and when m approach to one the state (4) become phase state.

Since we are concerned with some statistical properties of the state (4), therefore we devote the next section to consider some of the nonclassical properties. Precisely we discuss the phenomenon of squeezing as well as the correlation function. In Section **2** we discuss the quasi-probability distribution functions, namely the Wigner and Q-functions. Section **4** is devoted to consider the phase properties which is followed by Section **5** where our conclusion is given.

2 Nonclassical properties

A traditional task for the nonclassical properties is to consider the phenomenon of the squeezing as well as the Poissonian distribution. This can be discussed when one uses the usual definition for the quadrature variances as well as the Glauber second order correlation function, respectively. Therefore we devote this section to consider these phenomena in some details. For this reason we divide this section into two subsections and start with the phenomenon of squeezing.

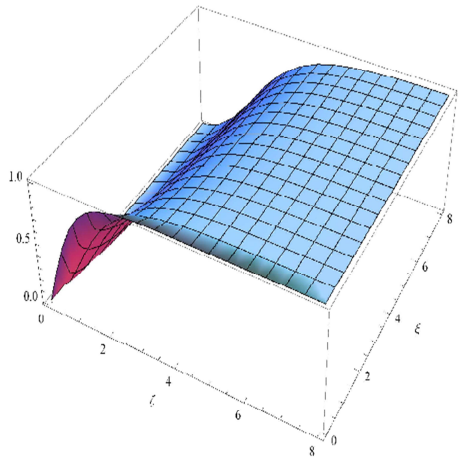

Fig. 1: The coefficient m against the variable ξ and ζ.

2.1 The squeezing phenomenon

It is well known that squeezing means reduction in the noise of an optical signal below the vacuum limit. The phenomenon has wide applications in optical communications networks and in the gravitational wave detection [19,20,21,22]. From mathematical point of view we can measure the squeezing if we calculate the Hermitian quadrature variances $\hat{X}$ and $\hat{Y}$. These quadrature operators satisfy the commutation relation $[\hat{X},\hat{Y}]=i\hat{C}$, where $\hat{C}$ may be an operator or C-number depending on which kind of squeezing we want to discuss. For the present state it is most likely to observe the phenomenon of the squeezing if we use the definition of the frequency sum squeezing. Therefore, to facilitate our discussion we introduce the frequency sum squeezing quadratures defined by

$$\hat{X}=\frac{\hat{a}\hat{b}+\hat{a}^{\dagger}\hat{b}^{\dagger}}{2},\qquad \hat{Y}=\frac{\hat{a}\hat{b}-\hat{a}^{\dagger}\hat{b}^{\dagger}}{2i} \tag{5}$$

which satisfy the commutation relation

$$\begin{gathered}[\hat{X},\hat{Y}]=i\hat{C},\\ \hat{C}=\frac{1}{2}(\hat{n}_a+\hat{n}_b+1)\end{gathered} \tag{6}$$

thus leading to the uncertainty relation:

$$(\Delta\hat{X})^2(\Delta\hat{Y})^2 \geq \frac{1}{4} < \hat{C} >^2 \tag{7}$$

The variance is given in terms of annihilation and creation operators expectation values by

$$\begin{aligned}\langle(\Delta\hat{X})^2\rangle &= \frac{1}{4}+\frac{1}{4}(2Re < \hat{a}^2\hat{b}^2 > +2 < \hat{n}_1\hat{n}_2 > + < \hat{n}_a+\hat{n}_b >) - \left(Re(< \hat{a}\hat{b} >)\right)^2 \\ \langle(\Delta\hat{Y})^2\rangle &= \frac{1}{4}+\frac{1}{4}(2 < \hat{n}_a\hat{n}_b > -2Re < (\hat{a}^2\hat{b}^2) > + < \hat{n}_a+\hat{n}_b >) + \left(Im(< \hat{a}\hat{b} >)\right)^2\end{aligned} \tag{8}$$

The model possesses $\hat{Y}$-quadrature frequency sum squeezing if the S-factor defined by

$$S(m) = \frac{\langle(\Delta\hat{Y})^2\rangle - 0.5 < \hat{C} >}{0.5 < \hat{C} >}, \tag{9}$$

has negative values.

In this case we note that frequency sum squeezing persists for a considerable for different values of q. It should be noted that the phenomenon of squeezing for this particular quadrature variances depends only on the value of q.

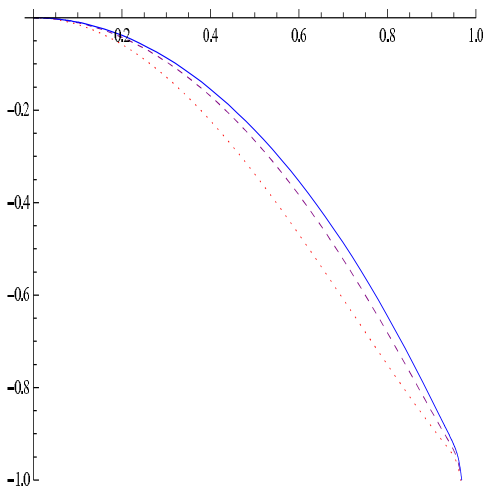

Fig. 2: The phenomenon of squeezing for the first quadrature Y and different values of q where the solid curve for $q = 1$, the dash curve for $q = 5$ and the dot curve for $q = 10$

To illustrate our discussion we have plotted figures (2) for $q = 1, 5$ and 10. Fig. (2) display the squeezing in the quadrature $S_y(m)$, where no squeezing can be seen in the region close to $m \simeq 0$, however the amount of squeezing starts to occur when the variable m develops. However, it is observed that frequency sum squeezing is absent in the quadrature $S_x(m)$. In general for large values of the q parameter, the amount of squeezing in the quadrature $S_y(m)$ increases as observed in Fig. (2).

2.2 The correlation function

We devote the present section to consider an example of the nonclassical effects that is the phenomenon of sub-Poissonian distribution. This phenomenon can be measured by photon detectors based on photoelectric effect. The importance of the study comes up as a result of several applications, e.g. quantum nondemolition measurement, which can be generated in semiconductor lasers [19] and in the microwave region using masers operating in the microscopic regime [23]. It is well known that, sub-Poissonian statistics is characterized by the fact that the variance of the photon number $\langle(\Delta\hat{n}_i(t))^2\rangle$ is less than the average photon number $\langle\hat{a}_i^\dagger(t)\hat{a}_i(t)\rangle = \langle\hat{n}_i(t)\rangle$. This can be expressed by means of the normalized second-order correlation function [24] as follows.

$$g_z^{(2)}(m) = \frac{\langle\xi,\zeta,q|\hat{n}_z(\hat{n}_z-1)|\xi,\zeta,q\rangle}{\langle\xi,\zeta,q|\hat{n}_z|\xi,\zeta,q\rangle^2}, \ \forall\ z = a,b \tag{10}$$

where

$$\begin{aligned}\langle\xi,\zeta,q|\hat{n}_a(\hat{n}_a-1)|\xi,\zeta,q\rangle &= \frac{q(q-1)(1-m^2)^2+2qm^2(1-m^2)+2m^4}{(1-m^2)^2}, \\ \langle\xi,\zeta,q|\hat{n}_a|\xi,\zeta,q\rangle &= q-1+\frac{1}{(1-m^2)},\end{aligned} \tag{11}$$

and

$$\begin{aligned}\langle\xi,\zeta,q|\hat{n}_b(\hat{n}_b-1)|\xi,\zeta,q\rangle &= \frac{2m^4}{(1-m^2)^2}. \\ \langle\xi,\zeta,q|\hat{n}_b|\xi,\zeta,q\rangle &= \frac{m^2}{(1-m^2)}\end{aligned} \tag{12}$$

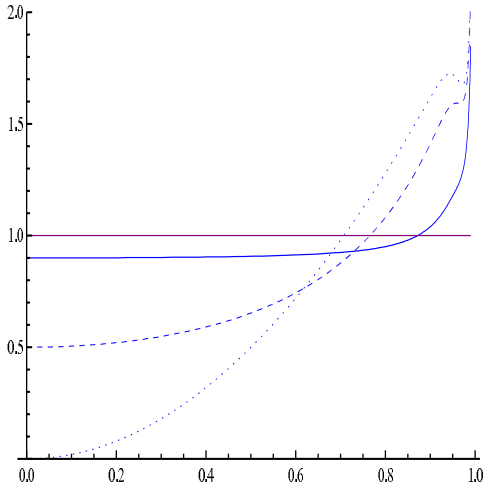

Fig. 3: The correlation function $g_z^{(2)}(\zeta)$ against the parameter m and for the first mode where $q = 1$ for (solid curve), $q = 2$ for (dot curve) and $q = 10$ for (dash curve).

The function $g_z^{(2)}(m)$ given by (10) for the mode z serves as a measure of the deviation from the Poissonian

distribution that corresponds to coherent states with $g_z^{(2)}(m)=1$. If $g_z^{(2)}(m)<1(>1)$, the distribution is called sub (super)-Poissonian, if $g_z^{(2)}(m)=2$ the distribution is called thermal and when $g_z^{(2)}(m)>2$ it is called super-thermal.

Before we go further let us point out that, in our examination for the case in which $q=0$, we find the two mode having the same behaviour, the correlation function $g_2^{(2)}(m)$ represents thermal state as expected from equation (12). It is to be observed that the state (4) for the first mode and for different values of the parameter $q=1,2,10$, starts full sub-Poisson distribution for large region consideration and the distribution increases gradually when the variable m develops and reach to Poissonian and super-Poissonian distribution see Fig. (3). Also we find that the function starts at $0,\frac{1}{2}$ and $\frac{9}{10}$ respectively. This is because it looks as that we have the Fock state $|\xi,\zeta,q\rangle=|q,0\rangle$ present in this case when $m\to 0$ so $g_a^{(2)}(m)=\frac{q-1}{q}$as shown in [16]. We note that the same behaviour can be seen on increasing the parameter q, however there is one main difference. The difference is that the maximum values of the correlation function on the start depends on the parameter q, so for large values of q the function $g_a^{(2)}(m)$ starts almost Poissonian. For a large value of m, the distribution reaches the thermal distribution as we get the limit $g_b^{(2)}(m)=2$ as depicted in Fig. (3) for $m\gg 1$.

3 Quasiprobability distribution

It is well known that there are three quasiprobability distribution functions: P-representation, W-Wigner, and Q-function [25]. These functions are regarded as important tools to provide insight into the nonclassical features of the radiation fields. In the meantime they have advantages and disadvantages connected with their use. As a marked disadvantage the P-function (which describes a quantum state in terms of the probability that the system is in a given coherent state) is highly singular or negative for quantum states with no classical analogues. While the Wigner function may become negative for some quantum states, but it has the considerable advantage for squeezed states that its contour map out the variances in the field quadratures. The Q-function is a positive-definite quasiprobability distribution, but its simple relation to anti-normal operator products makes it difficult to interpret in terms of conventional photon counting or squeezing measurements [26,27]. The s-parameterized characteristic function (CF) for the two-mode states is defined as follows

$$C(\lambda_1,\lambda_2,s)=Tr[\hat{\rho}\hat{D}(\lambda_1)\hat{D}(\lambda_2)]\exp\{\frac{s}{2}(|\lambda_1|^2+|\lambda_2|^2)\}, \tag{13}$$

With the s-parameterized quasi-probability distribution functions (QDF) for the two-mode case given by

$$F(\beta_1,\beta_2,s)=(\tfrac{1}{\pi^2})^2\int\int C(\lambda_1,\lambda_2,s)\exp(\lambda_1^*\beta_1+\lambda_2^*\beta_2-\lambda_1\beta_1^*-\lambda_2\beta_2^*)d^2\lambda_1 d^2\lambda_2, \tag{14}$$

We consider a phase space QDF for our states. To begin the state (4) will be written in the form

$$|\xi,\zeta,q\rangle=\sum_{n=0}^{\infty}B_n(\zeta,\xi)|q+n,n\rangle, \tag{15}$$

where

$$B_n(\zeta,\xi)=\sqrt{1-|m|^2}.m^n \tag{16}$$

It is clear that, the probability of finding $n+q$ photons in the 1^{st} mode, and n photons in the 2^{nd} mode in the state $|\xi,\zeta,q\rangle$ is given by

$$P(n+q,n)=|B_n(\zeta,f,q)|^2. \tag{17}$$

In what follows we consider the Wigner, and the Q-function and for this reason we have to evaluate the integral in equation (14) for $s=0$ and $s=-1$, respectively. This can be achieved if one manages to calculate the characteristic function. From equation (14) and after minor algebra we have

$$C(\lambda_1,\lambda_2,s)=\exp[\{-\tfrac{(1-s)}{2}\}(|\lambda_1|^2+|\lambda_2|^2)]\sum_{n=0}^{\infty}|B_n(\zeta,\xi)|^2L_{n+q}[|\lambda_1|^2]L_n[|\lambda_2|^2], \tag{18}$$

$$F(\beta_1,\beta_2,s)=(\tfrac{2}{\pi(1-s)})^2\exp[\tfrac{-2(|\beta_1|^2+|\beta_2|^2)}{(1-s)}]\sum_{n=0}^{\infty}\sum_{j=0}^{n+q}\sum_{k=0}^{n}|B_n(\zeta,\xi)|^2\binom{n+q}{j}\binom{n}{k}\times(\tfrac{-2}{(1-s)})^{j+k}L_j[\tfrac{2|\beta_1|^2}{(1-s)}]L_k[\tfrac{2|\beta_2|^2}{(1-s)}] \tag{19}$$

where $L_n^q(x)$ are the associated Laguerre polynomials given by

$$L_n^q(x)=\sum_{r=0}^{n}\binom{n+q}{n-r}\frac{(-1)^r}{r!}x^r \tag{20}$$

Having obtained the parameterized characteristic function, we are therefore in a position to discuss the Wigner, and Q-function. This will be exhibited in the next subsections

3.1 The Wigner function

To obtain the Wigner function $W(\alpha,\beta)$ we insert $s=0$ in equation (19) we obtain

$$W(\beta_1,\beta_2)=\tfrac{4}{\pi^2}\exp[-2(|\beta_1|^2+|\beta_2|^2)]\sum_{n=0}^{\infty}\sum_{j=0}^{n+q}\sum_{k=0}^{n}|B_n(\zeta,\xi)|^2\binom{n+q}{j}\binom{n}{k}\times(-2)^{j+k}L_j[2|\beta_1|^2]L_k[2|\beta_2|^2] \tag{21}$$

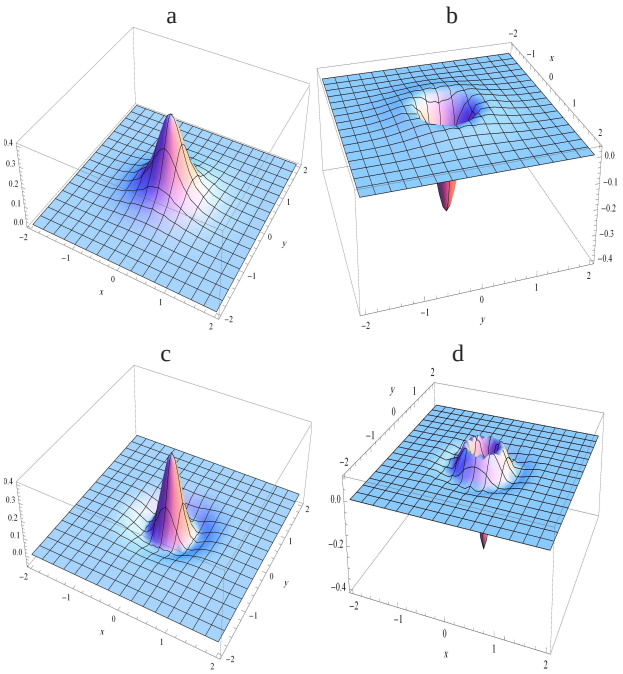

Fig. 4: The Wigner function against Re(α) and Im(α) for fixed values of $m = 0.5$. (a)-$q = 0$, (b)- $q = 1$, (c) $q = 2$, (d) $q = 5$

In order to visualize the behaviour of this function we choose a subspace in which $\beta_1 = \beta_1 = \alpha$ say. In figure (4) we have plotted the Wigner function against $Re(\alpha)$ and $Im(\alpha)$ for fixed values of $m = 0.5$. In the meantime we examined the function for the cases in which $q = 0, 1, 2$ and 5. When we consider the case in which $q = 0$, the function displays Gaussian shape with a symmetrical behaviour around the origin. In this case one can see a sharp peak centered at the middle of the bases, see Fig.(4a). As soon as we consider the value of the q-parameter and take $q = 1$, the peak of the function gets upside down and the nonclassical effect becomes pronounced. This is clear from Fig. (4b) where the negative values of the function are apparent. The spreading of Wigner over the plane is shown as q increases, this is seen for the case in which $q = 2$.

In this case the oscillatory behavior starts to appear for large values of the q-parameter. This indicates that the function gets more sensitive to the variation in the q-parameter and this of course reflects the change from Gaussian to non-Gaussian states; see Fig. (4c). For $q = 5$ the function displays the same shape, however, it changes its direction downward and exhibits negative values, see Fig.(4d). This indicates that the nonclassical behaviour appears only for the odd numbers of the q-parameter while it disappears for even numbers. This means that the q-parameter plays a role of changing the nonclassical behaviour.

3.2 The Q-function

Now if we set $s = -1$ in equation (19), then the Q-function has the form

$$Q(\beta_1,\beta_2) = (\tfrac{1}{\pi})^2 \exp[-(|\beta_1|^2+|\beta_2|^2)] \sum_{n=0}^{\infty} \sum_{j=0}^{n+q} \sum_{k=0}^{n} |B_n(\zeta,\xi)|^2 \binom{n+q}{j} \binom{n}{k} \times (-1)^{j+k} L_j[|\beta_1|^2] L_k[|\beta_2|^2] \tag{22}$$

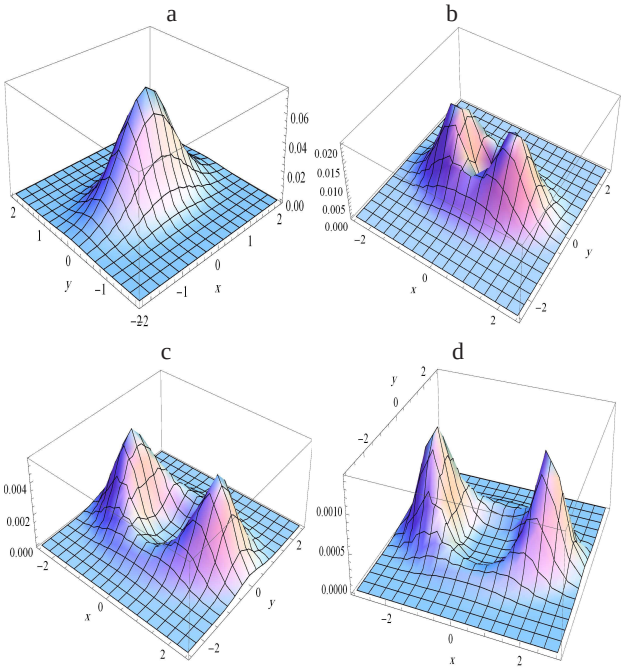

Fig. 5: The Q- function against $Re(\alpha)$ and $Im(\alpha)$ for fixed values of $m = 0.5$, (a)-$q = 0$, (b)- $q = 1$, (c) $q = 3$, (d) $q = 5$

where $\beta_1, \beta_2 \in \mathbb{C}$, with $|\beta_1\rangle$ and $|\beta_2\rangle$ being the usual coherent states. Since we have four variables associated with the real and imaginary parts of β_1 and β_2. Therefore, we confine ourselves to a subspace determined by $\beta_1 = \beta_2 = \beta$, [28]. In this subspace the Q-function for the state (4) is expressed in the equivalent form

$$Q(x,y) = \frac{1}{\pi^2} \exp[-2(x^2+y^2)] \times \left| \sum_{n=0}^{\infty} B_n(\zeta,\xi) \frac{\beta^{2n+q}}{\sqrt{(q+n)!n!}} \right|^2, \tag{23}$$

where $\beta = x + iy$.

Since the maximization or minimization of the Q-function depends on the parameter q. Therefore, our main task is to examine the behaviour of the Q-function due to the variation in the q-parameter. For this reason we plot $Q(\alpha)$ in figure (5) for different values of the

q-parameter keeping all other parameters unchanged as for the Wigner function case. For fixed $m = 0.5$ and for instance when we consider $q = 0$, the function exhibits Gaussian shape but with squeezing apparent on the contours of the base where it is elliptically shaped, see Fig.(5a). For $q = 1$, we note that the peak splits into two peaks but they are joined near of the base, see Fig.(5b). More increase in the value of q leads to a split of the two peaks and a spread out of the bases. Each base has a crescent like shape as shown clear for the cases in which $q = 3,5$, see Fig.(4c,d). It is also noted that there is a very slight difference between the heights of the peaks. This means that there is a slight asymmetry in the function shape which reflects the effect of the squeezing.

4 Phase properties

We devote this section to discuss the phase distribution for the present state. For this reason it is convenient to use the phase distribution formalism introduced by Barnett and Pegg [29,30]. It is well known that the phase operator is defined as the projection operator on a particular phase state multiplied by the corresponding value of the phase. Therefore, for the present state one can cast the Pegg-Barnett phases distribution function $P(\theta_1,\theta_2)$ in the following form:

$$P(\theta_1,\theta_2) = \frac{1}{4\pi^2}\sum_{n,m=0}^{\infty} B_n(\zeta,\xi)B_m^*(\zeta,\xi)\exp\{i(n-m)(\theta_2+\theta_1)\}. \tag{24}$$

In other word the phase distribution function can be rewritten in the form

$$P(\theta) = \frac{(1-m^2)}{4\pi^2}\left|\sum_{n=0}^{\infty} B(n)\exp[in\theta]\right|^2, \qquad -\pi \le \theta \le \pi \tag{25}$$

where $\theta = \theta_2 + \theta_1$ and the function is normalized according to $\int_{-\pi}^{\pi}\int_{-\pi}^{\pi} P(\theta_1,\theta_2)d\theta_1 d\theta_2 = 1$. As a result of the correlation between the two modes we find that, the phase distribution will depend on the sum of the phases of the two modes. In this context we have plotted in figures (6) the function $P_{\zeta,q}(\theta)$ against the angle $\theta = \theta_2 + \theta_1$ for a fixed value of $q = 3$ but for different values of the parameter m.

Here, we restrict our discussion to the cases in which $q = 3$ and $m = 0.3, 0.5$ and 0.7 where partial coherent phase states result and the phase distribution shows one-peak structure. This peak is centered at $\theta = 0$ with a symmetrical distribution around the central peak. For $m = 0.3$, it is observed that the function $P(\theta)$ starts at $P(-\pi) = 0.02$ for $m = 0.3$, 0.015 for $m = 0.5$ and 0.05 for $m = 0.7$, respectively, see Fig.(6). It is also noted that the value of the distribution function at $\theta = 0$ for the case in which $m = 0.3$, is smaller than that the case of $m = 0.7$. As one can see the range of the peak in this case is wider than that the case in which $m = 0.3$. In the meantime, the function $P(\theta)$ for a large value of the m-parameter the function $P(\theta)$ increases its maximum as observed in Fig.(6). It is to be noted that as $m \to 1$, the coherent phase state is realized and we get a delta function distribution.

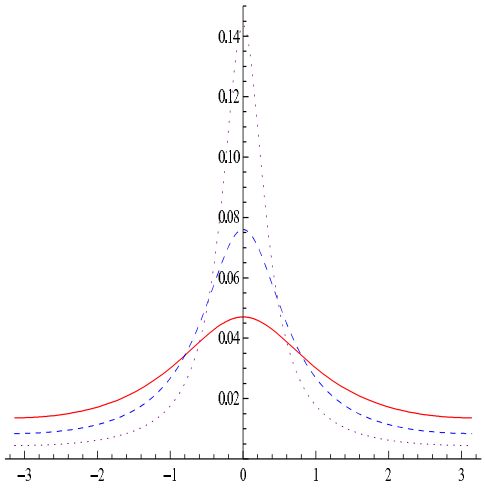

Fig. 6: The phase distribution $P(\theta)$ against θ for fixed $q = 3$ and the solid curve for $m = 0.3$, the dash curve for $m = 0.5$ and the dot for $m = 0.7$.

5 Conclusion

In the present paper we have introduced a new nonlinear entangled pair coherent state under a particular choice of the nonlinearity functions the resulting recurrence relation is solved and a feasible state is considered. For a particular definition of the quadrature variances, the phenomenon of squeezing is observed where the amount of the squeezing depends on the values of the m and q parameters. In the meantime we have employed the Glauber second order-correlation function to examine the nonclassical properties of the state. We have shown that the nonclassical as well as the classical behaviour are apparent in both modes for different values of m. However, the nonclassical effect is more pronounced in the first mode while the classical behaviour is pronounced in the first mode. We have also considered the quasiprobability distribution functions (the Wigner and Q-functions) where observation of nonclassical properties is reported for the odd values of the q-parameter. In the meantime the Q-function displays Gaussian behaviour and tends split up into two shapes as q increases. Finally we have examined the properties of the present state in terms of the phase distribution function introduced by Barnett and Pegg. In this case the function shown a symmetry peak around zero whatever the value of the m and q parameters. However, as the m-parameter increases

the maximum value of the function increases but without breaking the symmetry.

Appendix:

Here we shall briefly derive the state given by equation (4). To do so we use the equation (3)

$$\hat{a}_1\hat{a}_2 = (\mu\hat{a}\hat{b}f(\hat{n}_a)f(\hat{n}_b) + \nu f(\hat{n}_a)f(\hat{n}_b)\hat{a}^\dagger\hat{b}^\dagger - \sqrt{\mu\nu}(\hat{a}\hat{a}^\dagger\,(f(\hat{n}_a+1))^2 + \hat{b}^\dagger\hat{b}\,(f(\hat{n}_b))^2)), \tag{26}$$

where $\mu = \cosh^2\zeta$ and $\nu = \sinh^2\zeta$. Since the operators $\hat{a}\hat{b}$ and $\hat{a}^\dagger\hat{a} + \hat{b}\hat{b}^\dagger$ commute, therefore we can introduce a new state $|\phi\rangle$ which is simultaneously an eigenstates for both operators. In this case we have

$$|\phi\rangle = \sum_{n=0}^{q} C_n|q+n,n\rangle, \qquad \text{so that} \qquad \hat{a}_1\hat{a}_2|\phi\rangle = \xi|\phi\rangle. \tag{27}$$

Therefore we use equations (26) and (27) then the recurrence relation among the coefficients C_n is obtained in the form

$$\begin{aligned}&\mu\sqrt{(n+1)(q+n+1)}f(n+1)f(q+n+1)C_{n+1}\\ &+\nu\sqrt{n\,(q+n)}f(n)f(q+n)C_{n-1}\\ &-\sqrt{\mu\nu}((q+n+1)f^2(q+n+1)+nf^2(n))C_n = \xi C_n,\end{aligned} \tag{28}$$

Choosing $f(\hat{n}) = \frac{1}{\sqrt{\hat{n}}}$ and using equations (26) and (27), one can write the recurrence relation in the form

$$\mu C_{n+1} + \nu C_{n-1} - 2\sqrt{\mu\nu}C_n = \xi C_n \tag{29}$$

By using the transformation

$$C_n = (\frac{\nu}{\mu})^{\frac{n}{2}}S_n$$

The recurrence relation becomes

$$S_{n+1} + S_{n-1} - \beta S_n = 0$$

Where $\beta = 2 + \frac{\xi}{\sqrt{\mu\nu}}$, now we introduce the solution on the form

$$S_n = k^n, \text{ and } |k| < 1 \tag{30}$$

from which the characteristic equation of (29) takes the form,

$$k^2 - \beta k + 1 = 0, \tag{31}$$

as one can see the solution of equation (31) under the condition $|k| < 1$ is

$$k = \frac{\beta}{2} - \sqrt{(\frac{\beta}{2})^2 - 1}.$$

Whence we can write the new state in the form

$$\begin{aligned}|\phi\rangle &= |q,\zeta,\xi\rangle\\ |\xi,\zeta,q\rangle &= \sqrt{1-|m|^2}\sum_{n=0}^{\infty} m^n|q+n,n\rangle\end{aligned} \tag{32}$$

where $m = k\tanh\zeta$.

References

[1] P.A.M. Dirac, Principles of Quantum Mechanics, 4th ed.(Oxford University Press, Oxford) 1958.
[2] R. Glauber, Phys. Rev. **130**, 2529-2539 (1963).
[3] V.V. Dodonov,I.A. Malkin and V.I. Mank'o, Physica **72**, 597-618 (1973).
[4] J. Peřina, Quantum Statistics of Linear and Nonlinear Optical Phenomena (Kluwer Academic Publishers, Dordrecht) 1991.
[5] M. Paulina, Phys. Rev. A **44**, 3325-3330 (1991).
[6] M. Paulina, Phys. Rev. A**45**, (1992) 2044-2051 (1992).
[7] D. Stoler, B.E.A. Saleh and M.C. Teich Opt. Acta **32**, 345-355 (1985).
[8] A. Vidiella-Barranco and J.A. Roversi, Phys. Rev. A **50**, 5233-5241 (1994).
[9] A.-S.F. Obada, S.S. Hassan,R.R. Puri and M.S. Abdalla, Phys. Rev. A **48**, 3174-3185 (1993).
[10] M.S. Abdalla, M.H. Mahran and A-S.F. Obada, J. Mod. Opt. **41**, 1889-1902 (1994).
[11] M.H. Mahran and A-S.F. Obada, J. Mod. Optics **35** , 1847-1853 (1988).
[12] M.S. Abdalla, A.-S.F. Obada and M. Darwish, J. Opt. B: Quantum Semiclass.Opt.**7**, S695-S704 (2005).
[13] M.S. Abdalla, A.-S.F. Obada and M. Darwash, Phys. Scr.**77**, 055002 (2008).
[14] E.M. Khalil, J. Phys. A: Math. Gen. **39**, 11053-11064 (2006).
[15] G.S. Agrwal, Phys.Rev.Lett.**57**, 827830 (1986).
[16] A.-S.F. Obada, E.M. Khalil, Optics. Comm. **260**, 19-24 (2006).
[17] E.M. Khalil, Inter. J. of Theoretical Physics, **46**, 2816-2828 (2007).
[18] M.S. Abdalla, A-S.F. Obada and E.M. Khalil, IL Onuovo cement **125**, 1509-1528 (2010).
[19] J.H. Shapiro, H.P. Yuen, M.J.A. Machado, IEEE Trans. Inform. Theory IT, **25**, 179-192 (1979).
[20] M.J. Collett, C.W. Gardiner, Phys. Rev. A **30**, 1386-1391 (1984) 1386; M.J. Collett, R. Loudon, J. Opt. Soc. Am. B **4**, 1525-1534 (1987).
[21] C.M. Caves, B.L. Schumaker, Phys. Rev. A **31**, 3068-3092 (1985).
[22] C.M. Caves, Phys. Rev. D **23**, 1693-1708 (1981).
[23] G. Remoe, F. Schmidt-Kaler and H. Walther, Phys. Rev. Lett. A **293**, 2783-2786 (1990).
[24] R. Loudon, The Quantum Theory of Hight (Clarendon Press, Oxford, (1983).
[25] U. Leonhardt and H. Paul, Prog. Quant. Electr. **19**, 89-159 (1995).
[26] K. E. Cahill and R. J. Glauber, Phys. Rev. **177**, 1857-1881 (1969).
[27] N. Moya-Cessa and P.L. Knight, Phys. Rev. A **48**, 2479-2481 (1993).
[28] Hyo Seok Yi, B.A. Nguyen and J. Kim, J. Phys. A: Math. Gen. **37**, 11017-11036 (2004).
[29] S.M. Barnett and D.T. Pegg, Phys. Rev. A **34**, 3849-3854 (1986).
[30] S.M. Barnett and D.T. Pegg, Phys. Rev. A **39**, 1665-1675 (1989).